

Study of feed temperature effects on performance of a domestic industrial PSA plant

Ehsan Javadi Shokroo · Mohammad Shahcheraghi · Mehdi Farniaei

Received: 10 April 2014 / Accepted: 17 July 2014 / Published online: 13 August 2014
© The Author(s) 2014. This article is published with open access at Springerlink.com

Abstract The Parsian N₂-PSA industrial plant, situated in the southern pars zone of Iran, was studied numerically by mathematical modeling and numerical simulation. The model coupled PDEs are solved using fourth order Runge–Kutta scheme. In this work, we are dealing with the feed temperature and investigating its effect on the N₂ purity and recovery, which is known as an operating variable. Finally, the results of simulations showed that the feed temperature near to 25 °C is well suited to N₂ production with respect to its purity and recovery. In addition, as the feed temperature increases N₂ productivity decreases.

Keywords Pressure swing adsorption · Industrial plant · N₂ production · Numerical simulation · Carbon molecular sieve

Nomenclature

A_w	Wall cross-sectional area (cm ²)
AD	Adsorption step
B	L-F parameter (atm ⁻¹)
BD	Blow down step
cp_g	Gas heat capacities (cal/g.K)
cp_s	Pellet heat capacities (cal/g K)
cp_w	Wall heat capacities (cal/g K)

D_L	Axial dispersion coefficient (cm ² /s)
ED	Equalization to depressurization step
EP	Equalization to pressurization step
h_i	Internal heat-transfer coefficient (cal/cm ² K s)
h_o	External heat-transfer coefficient (cal/cm ² K s)
ΔH	Average heat of adsorption (cal/mol)
ID	Idle step
K	Parameter for the LDF model
K_L	Axial thermal conductivity (cal/cm s K)
L	Bed length (cm)
P	Total pressure (atm)
PP	Providing purge step
P_r	Reduced pressure (—)
PG	Purge step
PR	Pressurization step
q	Amount adsorbed (mol/g)
q^*	Equilibrium amount adsorbed (mol/g)
q_m	Saturated amount adsorbed (mol/g)
R	Gas constant (cal/mol K)
R_p	Radius of the pellet (cm)
R_{Bi}	Inside outside radius of the bed (cm)
R_{Bo}	Outside outside radius of the bed (cm)
t	Time (s)
T	Gas phase temperature (k)
T_{atm}	Temperature of the atmosphere (K)
T_w	Wall temperature (K)
u	Interstitial velocity (cm/s)
y_i	Mole fraction of species i in gas phase
Z	Axial distance (cm)

Greek letters

α	Particle porosity
ε	Voidage of the adsorbent bed
ε_t	Total void fraction
ρ_g	Gas density (g/cm ³)

E. J. Shokroo (✉) · M. Shahcheraghi · M. Farniaei
PART-SHIMI Company, Martyr Fahmideh Talent Foundation,
Campus of Knowledge Based Companies, 87, Mirzaye Shirazi,
71 888 41111 Shiraz, Fars, Iran
e-mail: ehsan.javadi@hotmail.com

ρ_p	Pellet density (g/cm ³)
ρ_B	Bulk density (g/cm ³)
ρ_w	Wall density (g/cm ³)

Subscripts

B	Bed
<i>i</i>	Component <i>i</i>
p	Pellet
g	Gas phase
s	Solid
w	Wall

Introduction

In general, three commercial methods are available for nitrogen purification, namely cryogenic, membrane technologies and pressure swing adsorption (PSA). PSA process is a wide operating unit for separation and purification of gases that operates based on capability of solid adsorption and selective separation of gases. The important operational parameter in this system is the pressure, and most industrial units operate at/or vicinity of the surrounding temperature. Today, the PSA process completely is known in a wide region of the processes, and this process was preferred in contrast to other conventional separation methods, especially for lower capacity and higher purity [23, 25, 33]. The nitrogen purification by pressure swing adsorption (N₂-PSA) system is well suited to rapid cycling, in contrast to other cyclic adsorption separation processes, and this has the advantage of reducing the absorbent inventory and therefore the capital costs of the system [23]. Use of PSA process to gas separation took place for the first time in 1958 by Skarstrom. He provided his recommended PSA cycles to enrich oxygen and nitrogen in air under the subject of heatless drier [30]. Thus, Skarstrom invented a two-bed PSA cycle with equalization step for oxygen production from air using zeolite 13X adsorbent in 1966 [31]. The main reasons for the success of this technology are many reforms that reached in this field and also is the new design and configuration for the cycles and devices [10, 16, 17, 29].

PSA process performance was strongly influenced by design parameters (such as: bed size, adsorbent physical properties, configuration and number of beds) and operating variables (such as: pressurization time, production time, purge time, feed flow rate, purge flow rate, production flow rate, temperature and/or pressure variations). So, this may be the maximum performance to obtain in terms of the best process variables. Thus, it is important that the behavior of the PSA operating variables was undertaking a review to know the optimum operating conditions. In recent years, use of this method was followed by

researchers as a more important separation technique in air separation.

In modeling a kinetically controlled PSA process, the key requirement is an adequate representation of the mass transfer kinetics. For the systems showing kinetic selectivity, the mass transfer resistance is usually in the micropores and both linear driving force (LDF) [11], 1987; [1, 14] and micropore diffusion [7, 28] models. Shin and Knaebel [28] assumed that the diffusivities remain constant, while Farooq and Ruthven [7] allowed for the concentration dependence of the micropore diffusivity in accordance with the chemical potential gradient as the driving force. Detailed studies of diffusion in microporous adsorbents reveal that, for both zeolites [5, 26] and carbon molecular sieves [3, 15], the micropore diffusivity varies strongly with sorbate concentration.

Fernandez and Kenney [9] provided a theoretical analysis and adaptation to the experimental results for the separation of oxygen and nitrogen from air by a single bed pressure swing adsorption. They have compared the analytical approximations with the results of the experiments, and concluded that the approximately analytical solution can predict the adsorption bed dynamics for short cycle time. These authors also have reported that the exact numerical solution is an efficient method in the modeling and numerical simulation of the adsorption bed dynamics, especially in the case of long cycle time. Hassan et al. [11] proposed a simple dynamic model for the O₂-PSA process based on linear mass transfer rate relations and Langmuir equilibrium equation. These authors have assumed that the pressure remains constant during the adsorption and desorption steps. Farooq et al. [8] proposed a kinetically dynamic model for the O₂-PSA process, in which the adsorption is controlled by equilibrium instead of kinetic. Their testing system was a Skarstrom cycle [30]. The advantage of the kinetically proposed model by these researchers for the PSA systems is that the effects of mass transfer resistance and axial dispersion can easily be evaluated. The considered system by the authors is a simple two-bed PSA Skarstrom system, but utilizing the model is not limited for the multi-bed systems which are commonly used in large-scale units. Farooq & Ruthven [6] suggested a linear driving force model (LDF) assuming frozen solid concentration during pressurization and blowdown steps to numerical simulation of air separation process by adsorption method using carbon molecular sieve (CMS). A fix bed under a four-step cycle was used in the PSA experiments. The cycle steps were the same as the steps of Skarstrom fundamental cycle: (1) high-pressure production, (2) blowdown, (3) purge with product and, (4) pressurization with feed. The authors have concluded that a good agreement is between the simple LDF model and the experimental results and, also the LDF model has a high

compatibility with the more complicated pore-diffusion model. Farooq & Ruthven [24] modeled the PSA process dynamic behavior for the nitrogen recovery using zeolite 5A, zeolite 13X, and CMS using the theoretical and experimental investigation. The LDF and pore-diffusion models were also used to compare the rate of mass transfer in the adsorption beds. The experiments were performed in a dual-bed system with two configurations: (1) the Skarstrom cycle and (2) the Self-purging modified cycle. The comparison between simulation results and experiments showed that the simple LDF model can predict the effect of process variables, but the complicated pore-diffusion model indicated a better adaptation to the experimental results. Farooq & Ruthven [7] suggested a pore-diffusion model for modeling the bulk two-component gas separation process using a PSA system based on Langmuir equilibrium and also considering concentration dependency for diffusion coefficient. The PSA system used by the authors was investigated in two configurations: (1) Skarstrom cycle and modified Skarstrom cycle with pressure equalization step and self-purging. The concentration dependency for diffusion coefficient of micropore was also examined. The concentration dependency has a large effect on cyclic steady state (CSS) performance. Budner et al. [2] improved a thermal non-equilibrium model for the multi-component adsorption process. They also have designed a software for the computation and simulation air separation process based on vacuum swing adsorption (VSA) technique using molecular sieve zeolite adsorbent. They have claimed that the developed and studied mathematical model using its software is able to design and optimize the VSA units for oxygen production. Mendes et al. [18] investigated a PSA system using zeolite 5A and Skarstrom cycle through simulations and experiments. They showed that the pressure increasing during pressurization step causes increasing dispersion in the PSA beds and finally results in decrease of product purity and recovery. Time reduction of depressurization in blowdown step down to 4 s does not affect on product purity and recovery. Taking the pressure equalization step in the Skarstrom cycle causes improvement of product purity and recovery. Mendes et al. [19] examined the PSA unit for oxygen separation from air using zeolite 5A through simulations and experiments. The mentioned PSA system was studied in two configurations as Skarstrom cycle and Skarstrom cycle with pressure equalization step. They showed that, as the production flow rate increases the product purity decreases; as the production step time increases the product purity reduces while its recovery increases. Shin et al. [27] found the optimal conditions for oxygen recovery and productivity using a two-bed PSA system with incomplete equalization step. According to their findings, use of the incomplete equalization step for PSA cycle is the leading cause of

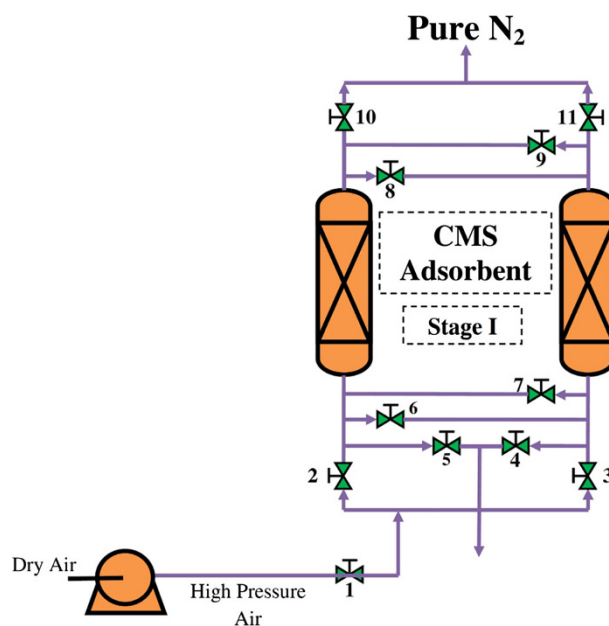


Fig. 1 Schematic diagram of Parsian N_2 -PSA industrial plant [22]

productivity improvement in the case of feed pressurization. The maximum productivity occurs using the incomplete equalization step, but its level is less than that for the case of feed pressurization. On the other hand, the maximum recovery always is obtained using complete equalization step. Cruz et al. [4] proposed a heuristic method to optimizing cyclic adsorption separation processes (PSA/VSA), in which the system acts based on Skarstrom cycle with pressure equalization step. They studied the various configurations for equalization step, and they found that bottom-to-bottom configuration is just efficient when adsorbent productivity is low and the Skarstrom cycle is used. The top-to-top configuration always is the most efficient in terms of product recovery and power consumption. Moghadaszadeh et al. [21] investigated different process variables such as production recovery, cycle time, production and purge flow rates on oxygen purity. They examined a four-bed PSA pilot consisting of seven steps to oxygen separation from air using zeolite 13X. These authors showed that the increasing purge flow rate maximized the product purity. Also, increasing cycle time is the leading cause of power consumption decrease, while power requirement will be increased. Mofarahi et al. [20] investigated a four-bed PSA consisting seven steps to oxygen separation from air using zeolite 5A. They reported that as long as the adsorption pressure increases from 4 to 6 bar, the oxygen purity and recovery increase. The PSA unit performance is improved at higher cycle times. When production flow rate increases oxygen recovery increases, while oxygen purity will be reduced.

The Parsian N_2 -PSA industrial plant, a two-bed PSA process, operates as modified Skarstrom cycle [23, 33].

Table 1 Model equations [23, 25, 33]

$$\frac{\partial C_i}{\partial t} - D_L \frac{\partial^2 C_i}{\partial z^2} + \frac{\partial(C_i u)}{\partial z} + \rho_p \cdot \left(\frac{1-\varepsilon}{\varepsilon}\right) \cdot \frac{\partial \bar{q}_i}{\partial t} = 0 \quad (1)$$

$$\frac{\partial C}{\partial t} - D_L \frac{\partial^2 C}{\partial z^2} + \frac{\partial(Cu)}{\partial z} + \rho_p \cdot \left(\frac{1-\varepsilon}{\varepsilon}\right) \cdot \sum_{i=1}^N \frac{\partial \bar{q}_i}{\partial t} = 0 \quad (2)$$

$$-K_i \frac{\partial^2 T}{\partial z^2} + \varepsilon \cdot \rho_g \cdot c_{p,g} \cdot \left(u \frac{\partial T}{\partial z} + T \frac{\partial u}{\partial z}\right) + (\varepsilon_i \cdot \rho_g \cdot c_{p,g} + \rho_B \cdot c_{p,s}) \cdot \frac{\partial T}{\partial t} - \rho_B \cdot \sum_{i=1}^N \left(\frac{\partial \bar{q}_i}{\partial t} \cdot (-\Delta \bar{H}_i)\right) + \frac{2h_i}{R_{B,i}} (T - T_w) = 0 \quad (3)$$

$$\rho_w \cdot c_{p,w} \cdot A_w \frac{\partial T_w}{\partial t} = 2\pi R_{B,i} h_i (T - T_w) - 2\pi R_{B,o} h_o (T_w - T_{am}); A_w = \pi (R_{B,o}^2 - R_{B,i}^2) \quad (4)$$

$$P(t) = a \cdot t^2 + b \cdot t + c \quad (5)$$

$$-\frac{dP}{dz} = a \cdot \mu \cdot u + b \cdot \rho \cdot u \cdot |u|; a = \frac{150}{4R_p^2} \cdot \frac{(1-\varepsilon)^2}{\varepsilon^2}; b = 1.75 \frac{(1-\varepsilon)}{2R_p \varepsilon} \quad (6)$$

$$q_i = \frac{q_{m,i} \cdot B_i \cdot P_i}{1 + \sum_{j=1}^N B_j \cdot P_j}; q_{m,i} = k_1 + k_2 \cdot T; B_i = k_3 \cdot \exp(k_4/T); n_i = k_5 + k_6/T \quad (7)$$

$$\frac{\partial \bar{q}_i}{\partial t} = \omega_i \cdot (\dot{q}_i - \bar{q}_i); \omega_i = \frac{15D_{ei}}{r_c^2}; \frac{15D_{ei}}{r_c^2} = C_i \cdot P_r^{0.5} \cdot (1 + B_i \cdot P_i)^2 \quad (8)$$

Figure 1 shows a schematic diagram of the process. The six-step process used is as follows: (1) co-current feed pressurization (PR) of a partially pressurized bed by a previous pressurizing pressure equalization step (EP); (2) high-pressure adsorption (AD) step; (3) counter-current depressurizing pressure equalization (ED) step; (4) counter-current blow down (BD) step; (5) counter-current purge with a light product (PG) step; (6) co-current EP step.

In this work, the Parsian N₂-PSA industrial plant is studied by mathematical modeling and numerical simulation. Furthermore, the effect of feed temperature on the plant performance (N₂ recovery and productivity) is investigated.

Mathematical model

To develop a mathematical model for a PSA system, the below main assumptions were given:

- Gas behaves an ideal gas.
- The flow pattern is described by the axially dispersed plug-flow model.
- Adsorbing properties throughout the tower would remain constant and unchanged.
- Radial gradient is to be negligible.
- Equilibrium equations for the components of the feed (N₂, O₂, Ar) can be expressed by three-component Langmuir–Freundlich isotherm.
- Mass transfer rate is expressed by a linear driving force equation.
- Thermal equilibrium between gas and solid phases is assumed.
- Pressure drop along the bed is calculated by the Ergun's equation.

The model equations for the bulk phase in the adsorption bed are written in Table 1 [12, 13, 32].

For the coupled PDEs problem, the well-known Danczkerts boundary conditions are applied [23, 25, 33]. The adsorption isotherm parameters and diffusion rate constant of N₂, O₂ and Ar over CMS are shown in Table 2. In Table 3, the characteristics of adsorbent and adsorption bed are shown.

Results and discussion

The fourth order Runge–Kutta scheme (for the time derivatives) and the implicit finite difference scheme (for the space derivatives) were used to solve the mathematical model that consisted of coupled partial differential equations.

The plant operating conditions data supplied by Parsian Co. can be found in Table 4 [22]. In this simulation study, the feed (air) components were assumed to be N₂, O₂ and Ar. To validate the simulation results, the results of this work first were compared with the plant data. Figure 2 shows the simulated N₂ purity as a function of feed flow rate, with N₂-PSA industrial plant data. This figure also shows as the feed flow rate increases the nitrogen purity decreases, which are in correspondence with other PSA simulations results [23, 25, 33]. In addition, as obvious in this figure, the simulation and presented model in this work predict the results of the plant data with a fairly high accuracy. The effect of feed temperature on N₂ purity and recovery is indicated in Fig. 3. It can be seen from this figure that the increasing of the feed temperature is the leading cause of a reduction in the N₂ purity and an increment in the N₂ recovery. The adsorption is an inherently exothermic phenomenal, so the decreasing of

Table 2 Equilibrium/rate parameters and heat of adsorption of N₂, O₂ and Ar on CMS [12]

Parameter	Component		
	N ₂	O ₂	Ar
$k_1 \times 10^3$ (mol/g)	23.63	15.27	20.42
$k_2 \times 10^3$ (mol/g k)	-0.0638	-0.00323	-0.00530
$k_3 \times 10^4$ (1/atm)	361	22.9	239.7
k_4 (k)	1,444	9,66.1	324.6
k_5 (-)	1.692	1.187	1.646
k_6 (k)	-270	-106	-238.2
Heat of adsorption, $-\Delta H_i$ (cal/mol)	3,197.532	3,297.828	3,398.124

Table 3 The characteristics of adsorbent and adsorption bed

Adsorbent [12]		Adsorption bed [22]	
Adsorbent	CMS	Length L (cm)	245
Type	Sphere	Inside radius, $R_{B,i}$ (cm)	80
Micropore diameter, R_p (cm)	3 A	Outside radius, $R_{B,o}$ (cm)	80.50
Particle density, ρ_p (g/cm ³)	0.9	Heat capacity of column, $C_{p,w}$ (cal/g k)	0.12
Bulk density, ρ_B (g/cm ³)	0.633	Density of column, ρ_w (g/cm ³)	7.83
Heat capacity, $C_{p,s}$ (cal/g k)	0.22	Internal heat-transfer coefficient, h_i (cal/cm ² k s)	9.2×10^{-4}
Particle porosity, α	0.30	External heat-transfer coefficient, h_o (cal/cm ² k s)	3.4×10^{-4}

Table 4 Industrial N₂-PSA operating condition [22]

Composition, mol (%)	Feed	Product	Tail
N ₂	79.00	99.99	N/A
O ₂	20.00	0.01	N/A
Ar	1.00	N/A	N/A
Pressure (bar)	7.00	6.50	1.00
Temperature (°C)	35.00	40.00	25.00
Flow rate (N m ³ /h)	319.800	N/A	N/A

the N₂ purity with the feed temperature has occurred in the normal way. In other hand, the incremental behavior of the N₂ recovery through the increasing of the feed temperature is caused by gas molar compression in the adsorption (AD) step, which means that the N₂ volume increases in the product stream. This figure shows that the feed temperature near to 25 °C is well suited to N₂ production in terms of its purity and recovery. Figure 4 depicts as the feed temperature increases N₂ productivity decreases. Productivity is defined as the ratio of moles of N₂ in the product stream to the kg of the adsorbent per cycle time. The cyclic partial concentration of N₂ at the top of the bed during a whole cycle is shown in Fig. 5. It is evident also from this figure that the process

performance (N₂ purity) is modified to correspond to lower feed temperature (25 °C) because of the cyclic concentration of N₂ placed at an upper level. In other words, it can reach the high pure N₂ (as the current purity in the plant) using higher feed flow rates when the feed temperature is near to 25 °C, which causes the increasing of N₂ recovery.

Conclusions

The Parsian N₂-PSA, located in the southern pars zone of Iran, has been simulated. The effect of feed temperature on the process performance is studied by a mathematical

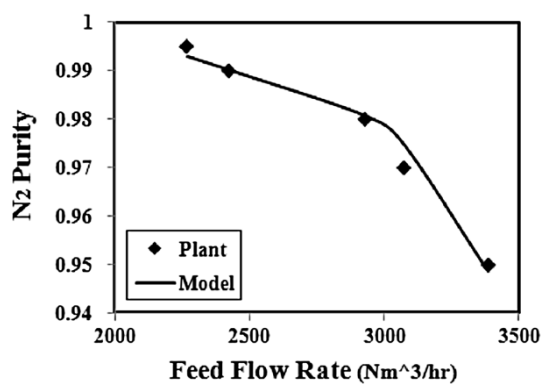


Fig. 2 Simulated purity and plant data of N₂-PSA industrial process as a function of feed flow rate

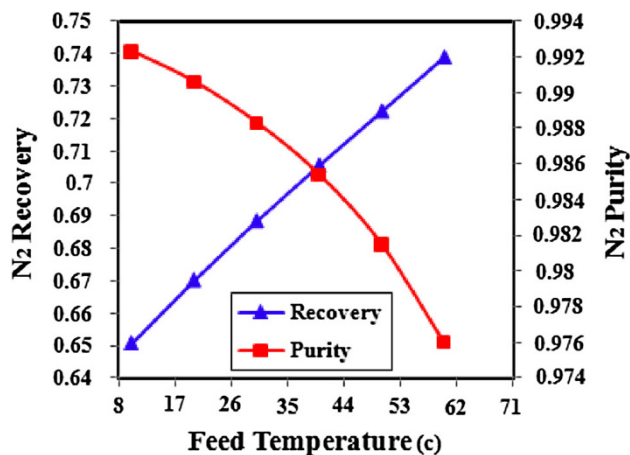


Fig. 3 N₂ purity and recovery as a function of feed temperature

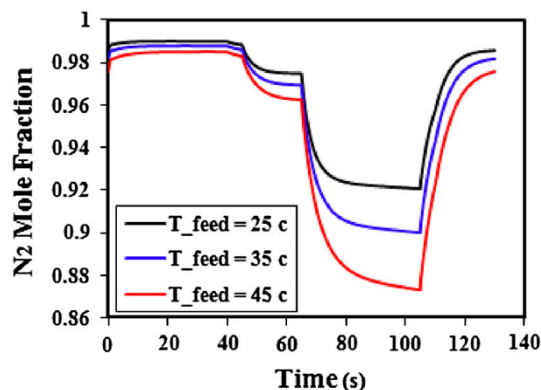


Fig. 5 Cyclic partial concentration of N₂ during a whole cycle at the top of the bed

modeling numerical simulation. The mathematical model in the gas phase takes into account the balances in energy, mass and momentum and the coupled PDEs are solved using fourth order Runge–Kutta scheme. Results showed

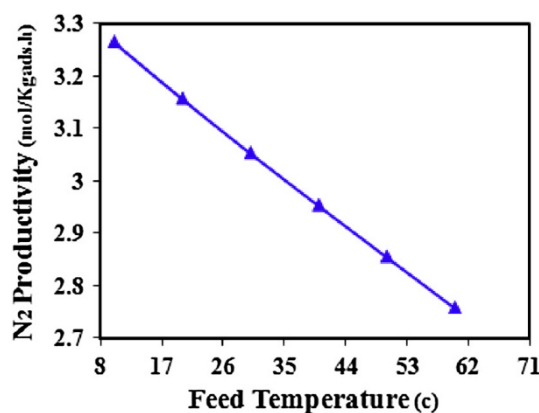


Fig. 4 Effect of feed temperature on the N₂ productivity

that the unit performance (in terms of N₂ purity and recovery) is in may well conditions when the feed temperature is near to 25 °C. Furthermore, as the feed temperature increases N₂ productivity decreases.

Acknowledgments The authors gratefully acknowledge the Parsian Gas Refining Co. for agreement with this research.

Open Access This article is distributed under the terms of the Creative Commons Attribution License which permits any use, distribution, and reproduction in any medium, provided the original author(s) and the source are credited.

References

- Ackley MW, Yang RT (1990) Kinetic separation by pressure swing adsorption: method of characteristics. *AIChE J* 36:1229–1238
- Budner Z, Dula J, Podstawa W, Gawdzik A (1999) Study and modeling of the Vacuum Swing Adsorption (VSA) process employed in the production of oxygen. *Ins Chem Eng*, 77, Part A, 405–412
- Chihara K, Suzuki M, Kawazoe K (1978) Concentration dependence of micropore diffusivities-diffusion of propylene in molecular sieving carbon 5A. *J Chem Eng Japan* 11:153–155
- Cruz P, Magalhaes FD, Mendes A (2005) On the optimization of cyclic adsorption separation processes. *AIChE J* 51:1377–1395
- Doetsch IH, Ruthven DM, Loughlin KF (1974) Sorption and diffusion of n-Heptane in 5A Zeolite. *Can J Chem* 52:2717–2724
- Farooq S, Ruthven DM (1990) A comparison of linear driving force and pore diffusion models for a pressure swing adsorption bulk separation process. *Chem Eng Sci* 45:107–115
- Farooq S, Ruthven DM (1991) Numerical simulation of a kinetically controlled pressure swing adsorption bulk separation process based on a diffusion model. *Chem Eng Sci* 46:2213–2224
- Farooq S, Ruthven DM, Boniface HA (1989) Numerical simulation of a pressure swing adsorption oxygen unit. *Chem Eng Sci* 44(12):2809–2816
- Fernandez G, Kenney CN (1983) Modeling of the pressure swing air separation process. *Chem Eng Sci* 38(6):827–834
- Fuderer A, Rudelstorfer E (1976) Selective adsorption process, US Patent 3,986,849

11. Hassan MM, Raghavan NS, Ruthven DM (1986) Air Separation by pressure swing adsorption on a carbon molecular sieve. *Chem Eng Sci* 41:1333–1343
12. Jee JG, Kim MB, Lee CH (2005) Pressure swing adsorption to purify oxygen using carbon molecular sieve. *Chem Eng Sci* 60:869–882
13. Jee JG, Park HJ, Haam SJ, Lee CH (2002) Effects of nonisobaric and isobaric steps on O₂ pressure swing adsorption for an aerator. *Ind Eng Chem Res* 41:4383
14. Kapoor A, Yang RT (1989) Kinetic separation of methane-carbon dioxide mixture by adsorption on molecular sieve carbon. *Chem Eng Sci* 44:1723–1733
15. Kawazoc K, Suzuki M, Chihara K (1974) Chromatographic study of diffusion in molecular-sieving carbon. *J Them Eng Jpn* 7:151–157
16. Malek A, Farooq S (1985) Hydrogen purification from refinery fuel gas by pressure swing adsorption. *AIChE J* 44:1985
17. Malek A, Farooq S (1997) Study of a six-bed pressure swing adsorption process. *AIChE J* 43:2509
18. Mendes AMM, Costa CAV, Rodrigues AE (2000) Analysis of nonisobaric steps in nonlinear bicomponent pressure swing adsorption systems: application to air separation. *Ind Eng Chem Res* 39:138–145
19. Mendes AMM, Costa CAV, Rodrigues AE (2001) Oxygen separation from air by PSA: modeling and experimental results part I: isothermal operation. *Sep Purif Tech* 24:173–188
20. Mofarahi M, Towfighi J, Fathi L (2009) Oxygen separation from air by four-bed pressure swing adsorption. *Ind Eng Chem Res* 48:5439–5444
21. Moghadaszadeh Z, Towfighi J, Mofarahi M (2008) Study of a four-bed pressure swing adsorption for oxygen separation from air. *Int J Chem Bio Eng* 1(3):140–144
22. Parsian GAS Refinement Co., N2-PSA plant, <http://www.nigc-parsian.ir/>
23. Ruthven DM (1984) Principle of adsorption and adsorption processes. John Wiley & Sons Inc, New York
24. Ruthven DM, Farooq S (1990) Air separation by pressure swing adsorption. *Gas Sep Purif* 4:141–148
25. Ruthven DM, Farooq S, Knaebel KS (1994) Pressure swing adsorption. VCH Publishers Inc, New York
26. Ruthven DM, Loughlin KF (1971) The sorption and diffusion of n-butane in linde 5a molecular sieve. *Chem Eng Sci* 26:1145–1154
27. Shin HS, Kim DH, Koo KK, Lee TS (2003) Performance of a two-bed pressure swing adsorption process with incomplete pressure equalization. *Adsorption* 6:233–240
28. Shin HS, Knaebel KS (1988) An experimental study of diffusion-induced separation of gas mixtures by pressure swing adsorption. *AIChE J* 34:1409–1416
29. Sircar S, Golden TC (2000) Purification of hydrogen by pressure swing adsorption. *Sep Sci Technol* 35:667
30. Skarstrom CW (1960) Method and apparatus for fractionating gaseous mixture by adsorption, US Patent, No. 2,944,627
31. Skarstrom CW (1966) Oxygen concentration process, US Patent, No. 3,237,377
32. Shokroo EJ, Shahcheraghi M, Farrokhzadeh A, Farniaei M (2014) The Iranian Jam Petrochemical's H₂-PSA enhancement using a new steps sequence table. *Pet Coal* 56(1):13–18
33. Yang RT (1987) Gas separation by adsorption processes. Butterworth, Reprinted by Imperial College Press, London